nature portfolio

https://doi.org/10.1038/s41550-021-01517-7

Supplementary information

Contemporary formation of early Solar System planetesimals at two distinct radial locations

In the format provided by the authors and unedited

Supplementary note

S1: Effects of changing key parameters

We discuss here how the results presented for the nominal simulation in the main text change if the values of the key parameters are varied.

S1.1: Prescription for centrifugal radius R_c.

Using the usual formulation from Ref.[51] as applied in previous studies[17-19], i.e. $R_c(t)$=10au $(M_{sun}(t)/M_\odot)^3$, the centrifugal radius expands very rapidly and the gas radial velocity becomes negative in the inner part of the disk in just 10 Kyr. Consequently, there is no pile-up of dust near 1au, even if α_{min} is reduced to 10^{-4} (as discussed below, a smaller value of α_{min} enhances planetesimal production). The sublimation/recondensation effect alone is not enough to reach the required critical dust/gas ratio for planetesimal formation. Consequently, planetesimals form only at the snowline. Assuming $R_c(t)=R_{c(0)}/(M_{sun}(t))^{0.5}$ as in the nominal simulation, but with $R_{c(0)}$=1au also does not allow the formation of planetesimals at the silicate-sublimation line (also for $\alpha_{min}=10^{-4}$) because in this case the radial velocity of the gas is never positive inward of 1.06au. Thus, it is essential that the centrifugal radius is significantly smaller than the distance where silicates sublimate in order to have a positive gas radial velocity and allow planetesimal formation at that location. The magnitude of the positive velocity also has importance. For instance, assuming $R_c(t)$=0.35au/$M_{sun}(t)$ (constant angular momentum of the infalling material), rocky planetesimal formation is significantly reduced because initially the gas falls at a larger distance (at t=0, when $M_{sun}(0)$= ½ $M_\odot$, $R_c(0)$ is bigger), so that the rate of radial expansion of the gas at the silicate sublimation line is reduced and turns negative ~20 Kyr earlier. The efficiency of rocky planetesimal formation can be restored to values similar to those of the nominal simulation by reducing the viscosity α_{min} in the disk.

It is also important that the positive radial velocity of the gas lasts long enough. For instance, if the infall rate is adjusted so that the star-disk system reaches 1$M_\odot$ in 170 Kyr and then is truncated as in Ref.[17-19], even assuming $R_c(0)$=0.35 au there would be no planetesimal formation near 1 au because the radial velocity of the gas turns negative as soon as the infall is suppressed, too early for a significant dust pile-up to be generated.

A small centrifugal radius requires efficient magnetic breaking to remove most of the angular momentum of the infalling gas. The efficiency of magnetic breaking depends on the intensity of the magnetic field, its coupling with the gas, the strength of ambipolar diffusion. Different simulations adopting different parameters depict different results. Ref.[52] shows streamers of gas feeding the disk at large distances from the central star, while in Ref.[27] the material falls very close to the central sink. It is possible that the situation may be different in reality from case to case. If magnetic breaking is not very efficient, very extended and massive disks form, which are prone to develop gravitational instabilities[52], while in presence of efficient breaking the resulting disks are rather small[27,53] that are never gravitationally unstable. Both cases are observed in the collection of extrasolar disks. Considerations based on the orbital distribution of trans-Neptunian objects suggest that the circumsolar disk was rather small, with a radial extension smaller than ~80 au[54]. Thus, it is reasonable to expect that magnetic breaking was strong, in the protosolar case.

S1.2: Prescription for α.

Two parameters are important in our prescription of the viscosity parameter: α_{min} and Q_{lim}. We have tested $\alpha_{min}=10^{-4}$ and, with the same Schmidt number Sc=10, we obtained an enhanced production of planetesimals near 1au, exceeding 30 $M_\oplus$. One could reduce Sc (proportionally to the ratio of α values at the time of rocky planetesimal formation in the nominal simulation, i.e. ~0.4 Myr) to reduce the total rocky planetesimal mass. Nevertheless, the two simulations (that with $\alpha_{min}=10^{-4}$, Sc=4 and the nominal one with $\alpha_{min}=5\times10^{-4}$, Sc=10) would not be equivalent: the disk would be colder than in the nominal simulation because of the reduced viscous heating; moreover the product αSc at t<0.4 Myr would be larger. The first effect shifts the ring of rocky planetesimals sunwards and the second effect reduces the amount of icy planetesimals formed at 5au, in favor of those formed at 3-4 au. The new distribution of planetesimals is shown in Fig.S1. Notice also that planetesimal formation at 1 au occurs ~0.1 Myr later than in the nominal simulation.

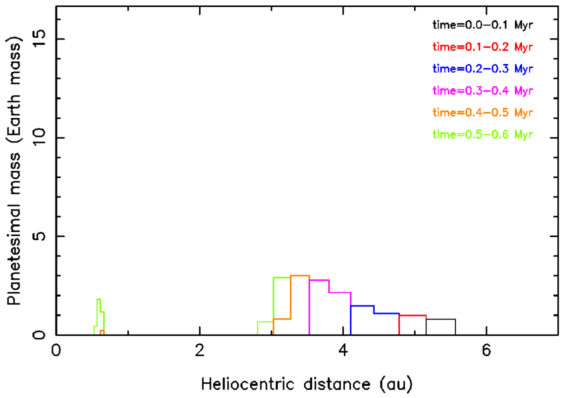

Fig S1: The same as Fig.3 of the main text, but changing α_{min} to10^{-4} and Sc to 6. Moreover, no information on the fraction of "early" disk material is provided here.

Concerning the value of Q_{lim} we tested the case $Q_{lim}=2$ recommended in Ref.[43]. A portion of the central disk (that with 2<Q<10) becomes less viscous more rapidly and consequently the gas has a reduced propensity to spread radially. The surface density of the disk is higher in the outer part and smaller in the inner part of the disk, and remains flat in the 3-7 au region (Fig. S2a). At t=1 Myr there is still a density of gas of ~500g/cm^2 at 6 au, which is about twice the value we find in our nominal simulation. The simulation with $Q_{lim}=2$ produces a much larger mass of planetesimals both at the silicate-sublimation line and at the snowline (Fig. S2b). The former is due to the fact that there is less gas in the inner part of the disk, so that the particles' Stokes number is bigger; the latter is due to the reduced viscosity in the snowline region.

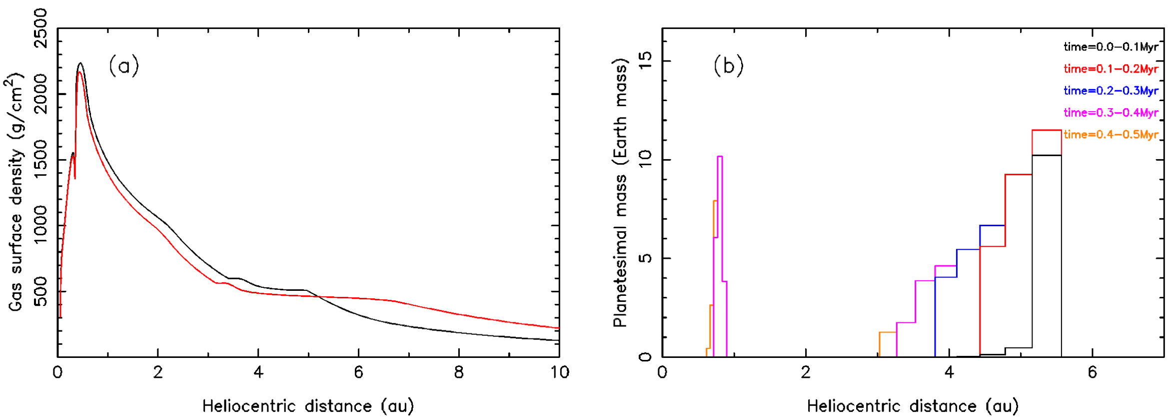

Fig. S2: (a) comparison between the disk's surface density distributions at t=0.5 Myr between the nominal simulation (black) and that with $Q_{lim}=2$ (red). (b) the planetesimals' radial mass distribution in the simulation with $Q_{lim}=2$. Compare with Fig.3 of the main text. No information on the fraction of "early" disk material is provided here.

S1.3: Planetesimal formation rate.
We compared the prescriptions given in Ref.[11] (nominal simulation) and Ref.[13] for the rate at which dust is converted into planetesimals when once $\rho_d/\rho_g>0.5$. Assuming $\varepsilon=0.1$ in the prescription of Ref.[13] suppresses the formation of rocky planetesimals, while it doubles the total mass of icy planetesimals. However, it is enough to reduce α_{min} to recover rocky planetesimal formation. For $\alpha_{min}=10^{-4}$ we obtain a total mass in rocky planetesimals that is 3 times that of our nominal simulation.

S1.4: Dependence on the planetesimals' total masses on parameters.
Extended Data Fig. 3 shows the total masses of icy and rocky planetesimals as a function of α_{min} for $Q_{lim}=2$ and 10. The total mass in rocky planetesimals increases sharply with decreasing α_{min} while the total mas sin icy planetesimals is less affected. This is because in our model most of icy planetesimals form early, when α is still much larger than α_{min}, particularly in the case $Q_{lim}=10$ in which the value of α is set by Q and not by the amount of material infalling onto the disk. Notice from Extended Data Fig. 3 that, while it is possible to have icy planetesimals and no rocky planetesimals (large α_{min}), the opposite is not true. Supposing that a population of planetesimals always forms a planet with a proportional mass, our model suggests that a rocky terrestrial or super-Earth planet should always be accompanied by an icy super-Earth or a giant planet (if the icy super-Earth becomes a seed for gas accretion). Observations seem to show a positive correlation between close-in super-Earths and distant giants[55,56]. The correlation between rocky super-Earths and more distant icy super-Earths is not confirmed because of the difficulty to detect distant super-Earths, but is a prediction of our model.

S1.5: Isotopic dichotomy.
The value of the time t_{dich} at which we switch from tracer #1 to tracer #2 affects the results in a straightforward manner. If we increase t_{dich} tracer #1 comes into the disk for a longer time. Hence its abundance relative to tracer #2 increases in both the icy and rocky planetesimals. The opposite is true if we decrease t_{dich}. A dichotomy of compositions between the two planetesimal populations would still be present but, if we fix the isotopic composition of tracer #1 to that carried by CAIs, the final isotopic properties of both CC and NC planetesimals would be less consistent with the measurements. Specifically, increasing t_{dich} shifts the yellow rectangle in Extended Data Fig. 4 to the right and above the solid and dash lines.

S1.6: Dust maximal sizes.
In our model we assume different maximal sizes for particles on opposite sides of the snowline and silicate-sublimation line. If we eliminate the size contrast at the snowline by setting the size of the rocky particles to 10cm (which is inconsistent with the current understanding of the fragmentation and bouncing barriers of silicate dust[8]) there is still planetesimal formation beyond the snowline, but with a reduced total mass (about 20 $M_\oplus$). If instead we eliminate the size contrast by reducing the size of icy particles to 5mm, planetesimal formation at the snowline is completely suppressed (also for $\alpha_{min}=10^{-4}$). This is not just because of the lack of size contrast on the two sides of the snowline, but also (and mostly) because of the very reduced Stokes number of the icy particles. A similar experiment, suppressing the size contrast at the silicate-sublimation line by reducing the size of silicate particles to 1mm, resulted in no planetesimal formation near 1au (also for $\alpha_{min}=10^{-4}$). Instead, if this size contrast is suppressed by increasing the size of refractory particles to 5mm, the formation of rocky planetesimals is impeded for $\alpha_{min}=5\text{x}10^{-4}$ but is recovered for smaller α_{min}. Thus, the size contrast between particles on opposite sides of a condensation line plays an important role and appears quite crucial for the formation of rocky planetesimals.

We also assumed more sophisticated recipes for the maximal size of particles. In one, we assumed that dust can grow only until its velocity dispersion $dv=(3\alpha/Sc\ St)^{1/2}$ reaches a threshold value. We nevertheless limit the maximal size of particles to be 10cm, 5mm and 1mm in the icy, silicate and refractory regimes, if the size limit provided by the velocity dispersion threshold is less stringent. We tested velocity thresholds of 1, 3 and 5 m/s. The limits at 3 and 5 m/s lead to qualitatively similar results. The total mass in icy planetesimals is reduced, by a factor up to 2, because the solid particles at the snowline are smaller than 10cm; instead the total mass of rocky planetesimals is increased by up to 75% because (i) the size limits of 5 and 1 mm are more severe than those given by the dispersion velocity and (ii) more material avoided to be trapped into icy planetesimals and drifted into the inner disk. However, assuming a threshold velocity of 1 m/s changes the results qualitatively. Planetesimal formation at the snowline is delayed because solid particles can become big enough only at a late time, when α has decreased sufficiently. Thus icy planetesimals form only when the snowline is at 3-4 au and their total mass is reduced to ~1/3. Rocky planetesimal formation still occurs, but their total mass is reduced to ~1/10 (it could be increases by lowering α_{min}). In the other recipe, we attempted to account for the new result that the sticking properties of ice depend on temperature[57]. Thus, we assumed that a maximal size D_{max}=10cm $(T/170K)^n$ for icy particles, with n=1,2,4. The result in terms of planetesimal formation does not change significantly. The particle size changes beyond the snowline, but because the temperature decays as $r^{-1/2}$ in the irradiation dominated regime, even for n=2 the decay in particle size is not very strong.

S1.7: <u>Sublimation/recondensation prescription at the snowline</u>.

In our work we assume complete evaporation of water above a fixed sublimation temperature (170K here). In reality water-vapor can co-exist with water-ice up to a maximum pressure, that depends on local temperature, the "saturating vapor pressure" [8,10,12]. So water vapor can subsist also beyond the snowline and some icy grain can survive also inward of the snowline. In principle this may change the surface density distribution of solids in the vicinity of the snowline, affecting planetesimal formation. To test the differences in the results between the two approaches, we use the code developed in Ref.[12] which accounts for partial pressure of vapor in the condensation/sublimation process, an option which can easily be removed for comparisons. The disk modeled in Ref.[12] is different from the one modeled here: it is colder and less massive, so that the snowline is much closer to the central star. Nevertheless we can simulate a situation analogue to the one investigated here if the diffusion coefficient in normalized coordinates at the snowline is the same in the two cases. The diffusion coefficient in normalized coordinates ($r=1$, $\Omega=1$) is $D=\alpha\, h^2/Sc$, where h is the disk's aspect ratio and Sc is the Schmidt number. For a given temperature (i.e. T=170K at the snowline) h is proportional to $r_{snow}^{1/2}$. In the code of Ref. [12] we assume $\alpha=10^{-3}$ and Sc=1; the snowline is at r_{snow}=1.4 au (h=0.037), and therefore $D=1.37\times10^{-6}$. We find the same in our disk at t=150,000y, when r_{snow}=5 au (h=0.07), $\alpha=2.8\times10^{-3}$ and Sc=10. Notice that at this time icy planetesimal formation is fully under way in our model.

Fig. S3 shows the results provided by the code in Ref.[12] if instantaneous sublimation/condensation is assumed (left panel) or the accurate calculation based on water vapor partial pressure is implemented (right panel). In the left panel, there is an abrupt transition between the water vapor density (dotted blue line) and icy grains density (solid blue line). In the right panel, the density of water vapor extends beyond the snowline (dashed-blue line). Nevertheless the density distribution of icy solids is very similar in both cases. This is because there is nevertheless a one-order-of-magnitude drop in the density of vapor at the snowline and the grains condensed there are allowed to diffuse radially.

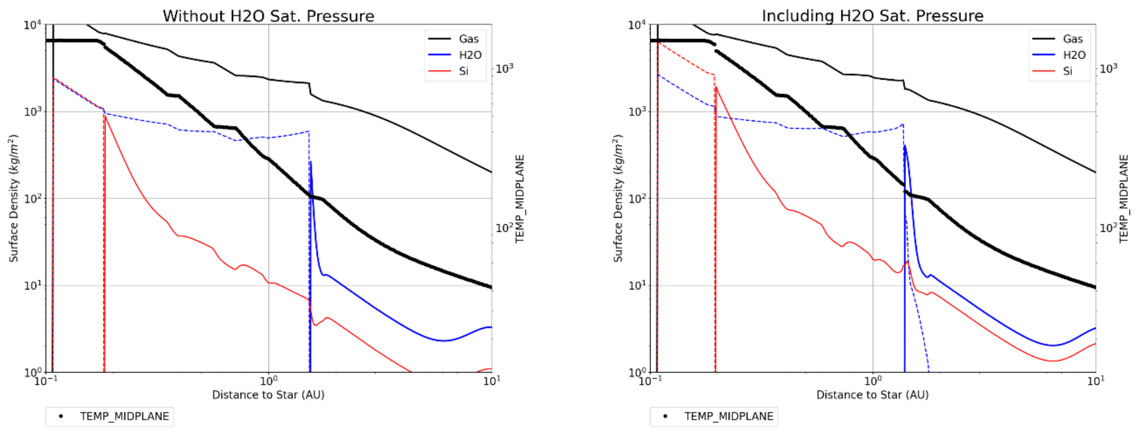

Fig. S3. The surface density of the disk (black thick line), of water (blue line: dotted for vapor and solid for ice) and silicate (red line) and temperature of the disk (black thin line) in the model of Ref.[12]. In this experiment the diffusion coefficient at the snowline is the same as in our model during icy planetesimal formation. In the left panel water vapor is turned instantaneously to solid at the snowline, while in the right panel water sublimation/recondensation is computed taking into account the partial pressure of water vapor. The distribution of ice turns out to be almost identical in the two cases, indicating that in case of significant diffusion the instantaneous recondensation of water at the snowline is a good approximation.

The situation would be different if D were much smaller (e.g. for $\alpha=10^{-4}$); in this case the distribution of solids would be less peaked beyond the snowline if the condensation rate were computed from the water vapor partial pressure. However, planetesimal formation is over in our model before that these conditions are met. Thus, we conclude that our simplified treatment of evaporation/condensation is adequate for our purposes.

S2: A trade-off between viscosity and gas density

The formation of planetesimals requires to find a sweet-spot in the (α,$\sum_g$) parameter space. A small value of α helps the sedimentation and the radial concentration of particles, but does not spread the gas of the disk efficiently. Thus $\sum_g$ decays over time more slowly and the larger density of gas reduces the particles' Stokes number, vanishing the positive effects of the reduced viscosity. A larger value of α reduces the density of gas, which enhances the particles' Stokes number, but increases the particle vertical stirring and radial diffusion. For these reasons it is important that α is large at the beginning of the disk's evolution -so to favor rapid disk spreading and density decay- and then decreases to small values, as in our model. A simulation where $\alpha=10^{-2}$ throughout the simulation as in Ref.[17-19] would not produce planetesimals, unless an extreme value of Sc is adopted, as in Ref.[9]. However, remember that α cannot become too small, otherwise the disk becomes too cold to form planetesimals near 1 au (given that the formation site of rocky objects is related to the location of the silicate sublimation line), unless a heating mechanism operates in the disk in addition to viscous dissipation. Ohmic dissipation may be such a mechanism[58].

S3: Condensation temperatures and the formation of refractory-rich bodies

In this work we have invoked the sublimation/recondensation of 50% of the non-volatile material (dubbed generically as *silicates*) at T=1,000K. In a previous publication[33] we found evidence in the meteoritical record for a similar separation of materials, that we called *refractory materials* and *residual condensates,* but with condensation temperatures above and below 1,400K respectively. The recondensation of silicate vapor beyond the T=1,000K line in this work reproduces the process of formation of the residual condensates invoked in Ref.[33] (see also Ref.[22]), but the temperatures (1,000K vs. 1,400K) do not match. The mismatch is more apparent than real because Ref.[33] showed that the temperature at which refractory elements and residual condensates need to be separated depends on the pressure in the disk and its C/O ratio; they showed it could be 1,060K for P=10^{-4} bar and C/O=1.0. In this work, if we had assumed a larger temperature for the sublimation of silicates, the ring of rocky planetesimals would have shifted somewhat towards the Sun. The new location can be deduced from the intersection of the disk's temperature curve in Fig. 1 for t=0.4 Myr with the required value of the temperature. Thus, restoring the ring near 1 au would require a hotter disk than the one produced in the reference simulation, possibly due to Ohmic dissipation[68].

A more conceptual difference is that Ref.[33] argued that the refractory grains formed refractory-rich planetesimals which ultimately contributed to forming a refractory-rich Earth. In this work, instead, the refractory grains never reach a solid/gas ratio large enough to trigger planetesimal formation. This is because the pressure bump generated by the drop in gas surface density in the inner part of the disk (Extended Data Fig. 1, S2a), associated with the increase in viscosity (Extended Data Fig. 2), is not sharp enough to trap mm-sized particles[59]. If this is correct, explaining the formation of a refractory-rich Earth requires invoking the evaporation of Si from warm planetary embryos with an initial enstatite chondrite-like (i.e. supra-solar) Si/refractory-element ratio[60].

S4: Formation of CAIs and other refractory condensates

In our model, following Ref.[23], we identify CAIs with condensates from early-infalling material. This identification is necessary to explain why CAIs have a solar isotopic composition for oxygen. Following this identification, our model implies that CAI formation lasted up to t_{dich}=20 Kyr. It has been argued that the CAI formation period may have last up to[71] 200 Kyr, but this prolonged interval likely includes later reprocessing of CAIs following their formation. Consistent with this, a bulk Al-Mg isochron for CAIs, as well as internal Al-Mg isochrons for the most primitive CAIs are consistent with a much shorter formation interval of ~20 Kyr or less[61].

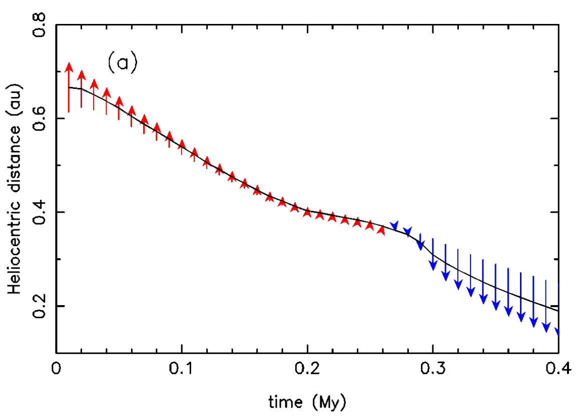

Fig.S4: The black curve shows the radial location where T=1,400K as a function of time. The arrows depict the radial displacement of the gas over 400y intervals. When arrows are red the gas cools during its radial motion, so condensation of refractory minerals is possible. The opposite is true when arrows are blue. The timescale over which condensation occurs (here 0.2 Myr) increases (decreases) if the assumed value of the centrifugal radius $R_c(0)$ is decreased (increased).

However, in our model the condensation of refractory minerals continues as long as the gas has a positive radial flow across the T=1,400 K line, i.e. for 0.2 Myr (Fig.S4). Thus our model implies the existence of grains with a CAI-like chemical composition but a NC isotopic composition. Refractory grains are not identified directly in NC chondrites, but they are expected to have been reprocessed in the formation of Al-rich chondrules. The isotopic analysis of these chondrules[62] revealed no isotopic anomalies pointing towards those of CAIs. This suggests that refractory grains with a NC isotopic composition indeed formed in the inner disk, in agreement with our model.

S5: Formation of late planetesimals: an outlook

This paper addresses the formation of early planetesimals, accreted in the first ½ Myr and related to iron meteorite parent bodies. The meteorite record, however, shows that there are also planetesimals that formed significantly later, such as the parent bodies of chondrites, whose formation times are constrained to be at least 2 Myr after CAI by the analysis of the ages of individual chondrules[63]. Like the parent bodies of all meteorites, those of chondrites are today in the asteroid belt, but originally they may have formed elsewhere, e.g. near 1 au for the NC chondrites[64] and beyond Jupiter for the CC chondrites[65,66,16], i.e. more or less in the same place where our early planetesimals form. The Kuiper belt objects also appear to have formed late, given that those with diameter D<700 km have a low bulk density implying the lack of internal differentiation[67]; they definitely formed beyond the location of our first icy planetesimals, up to about 45 au. Our model is not appropriate to discuss the formation of late planetesimals because we assume that all the dust in a radial bin has a unique size. Due to the lack of small dust strongly coupled with the gas, all the solid material in our model drifts towards the Sun quite rapidly. By 1 Myr, basically all the particles that have not been incorporated into planetesimals have drifted to the inner edge of the disk. Thus, there is no material left to form late planetesimals. Studying the formation of late planetesimals requires to consider that a significant fraction of the mass remains for long time stored in small particles that have a limited radially drift, as in Ref.[68]. It also requires to account for the formation of Jupiter, to block the radial drift of outer solar system particles as they grow in size and the photo-evaporation of the gas[69], in order to eventually increase the dust/gas ratio above the planetesimal-formation threshold. All these features are not present in our model and will be the object of future developments.

The formation of NC chondrites is even more complex. The fact that NC chondrites and NC irons have very similar isotopic properties requires little-to-no contamination from CC dust over millions of years. One possibility is that Jupiter forms at the same time as the NC iron meteorite parent bodies (~0.4 Myr in our model). In this case, the early/late material ratio in the inner solar system would be frozen at the NC value because the Jupiter's barrier prevents the penetration of new CC dust from the outer disk. However, the preservation of the material not incorporated in the first NC planetesimals until the chondrite formation time is problematic. In a low viscosity disk, Jupiter may form rings inwards of its orbital radius[70], possibly helping the preservation of dust. Another possibility is that the material that forms the NC chondrites is generated as debris in collisions among the first NC planetesimals. There is indeed a growing literature on the possibility that chondrules are collisional debris[36,71,72]. In this case the isotopic similarity between NC chondrites and irons would be obvious, because the two are genetically linked. In this case Jupiter would not need to form at the same time of NC iron meteorite parent bodies. It would just need to form at a generic time prior to NC chondrite formation, in order to keep the inner solar system clean of CC dust when such formation happened.

Supplementary references

[51] Shu, F.H. 1977. Self-similar collapse of isothermal spheres and star formation. The Astrophysical Journal 214, 488–497. Doi :10.1086/155274

[52] Kuffmeier, M., Frimann, S., Jensen, S.~S., Haugbolle, T. 2018. Episodic accretion: the interplay of infall and disc instabilities. Monthly Notices of the Royal Astronomical Society 475, 2642–2658. doi:10.1093/mnras/sty024

[53] Hennebelle, P., Commercon, B., Lee, Y.-N., Charnoz, S. 2020. What determines the formation and characteristics of protoplanetary discs?. Astronomy and Astrophysics 635. doi:10.1051/0004-6361/201936714

[54] Kretke, K.A., Levison, H.F., Buie, M.W., Morbidelli, A. 2012. A Method to Constrain the Size of the Protosolar Nebula. The Astronomical Journal 143. doi:10.1088/0004-6256/143/4/91

[55] Zhu, W., Wu, Y. 2018. The Super Earth-Cold Jupiter Relations. The Astronomical Journal 156. doi:10.3847/1538-3881/aad22a

[56] Bryan, M.L. and 6 colleagues 2019. An Excess of Jupiter Analogs in Super-Earth Systems. The Astronomical Journal 157. doi:10.3847/1538-3881/aaf57f

[57] Musiolik, G., Wurm, G. 2019. Contacts of Water Ice in Protoplanetary Disks-Laboratory Experiments. The Astrophysical Journal 873. doi:10.3847/1538-4357/ab0428

[58] Béthune, W., Latter, H. 2020. Electric heating and angular momentum transport in laminar models of protoplanetary discs. Monthly Notices of the Royal Astronomical Society 494, 6103–6119. doi:10.1093/mnras/staa908

[59] Ueda, T., Flock, M., Okuzumi, S. 2019. Dust Pileup at the Dead-zone Inner Edge and Implications for the Disk Shadow. The Astrophysical Journal 871. doi:10.3847/1538-4357/aaf3a1

[60] Young, E.D. and 6 colleagues 2019. Near-equilibrium isotope fractionation during planetesimal evaporation. Icarus 323, 1–15. doi:10.1016/j.icarus.2019.01.012

[61] MacPherson, G.J., Kita, N.T., Ushikubo, T., Bullock, E.S., Davis, A.M. 2012. Well-resolved variations in the formation ages for Ca-Al-rich inclusions in the early Solar System. Earth and Planetary Science Letters 331, 43–54. Doi :10.1016/j.epsl.2012.03.010

[62] Ebert, S. and 6 colleagues 2018. Ti isotopic evidence for a non-CAI refractory component in the inner Solar System. Earth and Planetary Science Letters 498, 257–265. doi:10.1016/j.epsl.2018.06.04

[63] Villeneuve, J., Chaussidon, M., Libourel, G. 2009. Homogeneous Distribution of 26Al in the Solar System from the Mg Isotopic Composition of Chondrules. Science 325, 985. doi:10.1126/science.1173907

[64] Raymond, S.N., Izidoro, A. 2017. The empty primordial asteroid belt. Science Advances 3, e1701138. doi:10.1126/sciadv.1701138

[65] Walsh, K.J., Morbidelli, A., Raymond, S.N., O'Brien, D.P., Mandell, A.M. 2011. A low mass for Mars from Jupiter's early gas-driven migration. Nature 475, 206–209. doi:10.1038/nature10201

[66] Raymond, S.N., Izidoro, A. 2017. Origin of water in the inner Solar System: Planetesimals scattered inward during Jupiter and Saturn's rapid gas accretion. Icarus 297, 134–148. doi:10.1016/j.icarus.2017.06.030

[67] Brown, M.E. 2013. The Density of Mid-sized Kuiper Belt Object 2002 UX25 and the Formation of the Dwarf Planets. The Astrophysical Journal 778. doi:10.1088/2041-8205/778/2/L34

[68] Charnoz, S., Taillifet, E. 2012. A Method for Coupling Dynamical and Collisional Evolution of Dust in Circumstellar Disks: The Effect of a Dead Zone. The Astrophysical Journal 753. doi:10.1088/0004-637X/753/2/119

[69] Carrera, D., Gorti, U., Johansen, A., Davies, M.B. 2017. Planetesimal Formation by the Streaming Instability in a Photoevaporating Disk. The Astrophysical Journal 839. doi:10.3847/1538-4357/aa6932

[70] Bae, J., Nelson, R.P., Hartmann, L. 2016. The Spiral Wave Instability Induced by a Giant Planet. I. Particle Stirring in the Inner Regions of Protoplanetary Disks. The Astrophysical Journal 833. doi:10.3847/1538-4357/833/2/126

[71] Johnson, B.C., Minton, D.A., Melosh, H.J., Zuber, M.T. 2015. Impact jetting as the origin of chondrules. Nature 517, 339–341. doi:10.1038/nature14105

[72] Choksi, N., Chiang, E., Connolly, H.C., Gainsforth, Z., Westphal, A.J. 2021. Chondrules from high-velocity collisions: thermal histories and the agglomeration problem. Monthly Notices of the Royal Astronomical Society 503, 3297–3308. doi:10.1093/mnras/stab503

Supplementary Table 1: HSE concentrations (ppm) for bulk iron meteorite cores and chondrites

	Re	Os	Ir	Ru	Pt	Reference
CI	40.7	491	462	688	943	[73]
Average OC	58.4	679	585	880	1185	[74]
Average EC	55.9	637	583	873	1186	[74]
CC irons						
IIC	280	3350	3050	4340	6070	[75]
IID	1100		10500		17400	[76]
IIF	355	4200	4200	6800	8200	[35]
IVB	2800	37000	27000	27400	29500	[77]
NC irons						
IC			2330			[34]
IIAB			3300			[78]
IIIAB			2100			[78]
IVA	295	3250	2700	3900	5900	[79]

Supplementary Table 2: Core mass fractions of NC and CC iron parent bodies

Iron meteorite group	Core mass fraction
CC irons	
IIC	0.15
IID	0.05
IIF	0.11
IVB	0.02
NC irons	
IC	0.25
IIAB	0.18
IIIAB	0.28
IVA	0.21

References :

[73] Horan, M. F., Walker, R. J., Morgan, J. W., Grossman, J. N. & Rubin, A. E. Highly siderophile elements in chondrites. *Chem. Geol.* **196**, 5-20, (2003).

[74] Walker, R. J. Highly siderophile elements in the Earth, Moon and Mars: Update and implications for planetary accretion and differentiation. *Chem Erde-Geochem.* **69**, 101-125, (2009).

[75] Tornabene, H. A., Hilton, C. D., Bermingham, K. R., Ash, R. D. & Walker, R. J. Genetics, age and crystallization history of group IIC iron meteorites. *Geochim. Cosmochim. Acta* **288**, 36-50, (2020).

[76] Wasson, J. T. & Huber, H. Compositional trends among IID irons; their possible formation from the P-rich lower magma in a two-layer core. *Geochim. Cosmochim. Acta* **70**, 6153-6167, (2006).

[77] Walker, R. J. *et al*. Modeling fractional crystallization of group IVB iron meteorites. *Geochim. Cosmochim. Acta* **72**, 2198-2216, (2008).

[78] Chabot, N. L. Sulfur contents of the parental metallic cores of magmatic iron meteorites. *Geochim. Cosmochim. Acta* **68**, 3607-3618, (2004).

[79] McCoy, T. J. *et al*. Group IVA irons: New constraints on the crystallization and cooling history of an asteroidal core with a complex history. *Geochim. Cosmochim. Acta* **75**, 6821-6843, (2011).